



**NPL Polarized Source Group  
Technical Note # 90-3A**

**Cleaning and Anodizing GaAs**

**B. M. Dunham**

**July 22, 1992**

university of illinois at urbana-champaign  
nuclear physics laboratory  
department of physics



# Cleaning and Anodizing GaAs

In this note we document a variant on the procedures that have been developed for cleaning and anodizing bulk GaAs samples for the polarized source. They are based largely on SLAC procedures that are documented in Technical Note # 90-3. The variations presented here are appropriate for "batch-processing" of three to four chips at a time. Refer to the original note for additional information. As was the case in the original note, we reproduce the paper by Schwartz that was the basis of the SLAC anodization procedure and a SLAC internal memorandum by T. Roder on measurements of the thickness of the anodization layer that results from this procedure as appendices. Additional appendices provide information on the cleaning of the NPL deionized water system, on the cleaning of glassware, and on the preparation of the necessary solutions.

## Materials necessary to etch 3-4 chips

Equipment	Chemicals <sup>†</sup>
1 1000 ml Pyrex Beaker	Methanol
3 400 ml Pyrex Beaker	Acetone
3 600 ml Pyrex Beaker	1,1,1 Trichloroethane
1 100 ml Pyrex Beaker	Hydrofluoric acid
3 400 ml poly tripour beaker	Sulfuric acid
1 poly basket	Phosphoric acid
1 stainless steel tweezers	30% hydrogen peroxide
1 teflon coated tweezers	Ammonium hydroxide
1 glass thermometer	Sodium Hydroxide pellets
1 hot plate	Deionized water (see Appendix C)
1 6 inch length of pure platinum wire (any convenient diameter)	
1 large Pyrex dish for ice	
1 large poly spill tray	
1 pair of eye protection with splash guards	
1 chemical resistant lab coat	
1 pair of chemical resistant gloves	
1 scale (accurate to 0.1 grams or better)	
1 bag of crushed ice	
pure aluminum foil	
Alconox soap	

<sup>†</sup> All chemicals should be electronic grade or better.

## Procedure

1. Degrease Wafers:
  - (a) Place three to four GaAs wafers in the nalgene basket, face up.
  - (b) Pour enough trichloroethane into a 600 ml beaker to cover the basket.
  - (c) Ultrasonically clean for 15 minutes at low power.
  - (d) Repeat steps 2 and 3 using acetone, then methanol.
  - (e) Repeat degreasing procedure twice.
2. Prepare Etching Solutions (see Appendix E)
3. Etch Wafers (see notes on following page):
  - (a) Place the three etching solutions in a nalgene spilltray. A separate beaker with deionized water should be nearby. The  $H_2SO_4$  etching solution should be on a hotplate adjusted to maintain the solution at 50 C, and the NaOH temperature should be maintained at 30 C.
  - (b) Remove the basket containing the crystals from the methanol and rinse with deionized water straight from the dispenser.
  - (c) Slowly lower the basket into the  $H_2SO_4$  solution.
  - (d) Etch for 3 minutes, face up, agitating occasionally to prevent surface bubble formation. Make sure that the solution is maintained at 50 C.
  - (e) Slowly remove the basket from the  $H_2SO_4$  solution, rinsing it and the crystals thoroughly and continuously with deionized water as you transfer them to the HF etch.
  - (f) Slowly lower the basket into the HF. Etch for 5 minutes, agitating occasionally.
  - (g) Slowly remove the basket from the HF, rinsing it and the crystals thoroughly and continuously with deionized water as you transfer them to the NaOH solution.
  - (h) Carefully lower the basket into the NaOH, etch for 1 minute, agitating occasionally. Maintain the solution temperature at 30 C.
  - (i) Remove the basket and rinse it and the crystals thoroughly and continuously with deionized water while transferring them to a beaker filled with deionized water.
  - (j) Lower basket into deionized water.
  - (k) Leave the chips on the deionized water and begin the anodization process described below. You will do the anodization one chip at a time. Complete the anodization of all the chips as quickly as possible so that the chips spend the minimum possible time in the water beaker.

#### Notes for the etching steps.

- Do not expose surface to air during each of the etching steps.
- Start with new glassware which you leach the first time with boiling deionized water (see appendix D).
- Use electronic grade chemicals; be sure 30%  $H_2O_2$  is fresh.
- Do not leave GaAs in  $H_2O$  longer than absolutely necessary.
- Mix all etches fresh (see Appendix E). Prepare all items beforehand.

#### 4. Anodize Wafers (see notes on following page):

- (a) Begin with a 100 ml Pyrex beaker that has been cleaned following the procedure outlined in Appendix D, and then rinsed three times with distilled water in the ultrasonic cleaner.
- (b) Prepare 1/2 liter of 2.8 ph phosphoric acid solution (made by adding 3-5 drops of acid to 500 ml of deionized water).
- (c) Sheath the ends of a pair of stainless steel tweezers with pure aluminum.
- (d) Form a loop about the size of a chip with the platinum wire and suspend it from the side of the 100 ml beaker so it is 1/4 - 1/2 an inch from the bottom.
- (e) Place the tweezers in the beaker and fill it with the phosphoric acid solution. (Do not fill it past the top of the aluminum sheath on the tweezers.)
- (f) Apply a negative 60-75 Vdc to the wire and ground the tweezers, let it run until the current stabilizes.
- (g) Remove the tweezers and scrape off a bit of the blue anodization at the tip of the tweezers; this provides good electrical contact with the chip.
- (h) Replace the phosphoric acid solution in the 100 ml beaker with fresh solution (again keeping the liquid level below the top of the aluminum sheath on the tweezers).
- (i) Under water, transfer a chip to the tweezers, and then transfer it to the 100 ml beaker. (Make sure the chip is face up and under the platinum loop.) **Caution: Do not let the tweezers touch the platinum wire.**
- (j) Apply a negative 40-50 Vdc to the wire to begin the anodization process; monitor the current, and continue the anodization until the current has stabilized at its minimum value for at least one minute and no new gas bubbles are formed on the surface of the GaAs, indicating that the anodization is complete.
- (k) Remove the GaAs wafer to a second beaker and rinse in five changes of deionized  $H_2O$  with agitation, face up. Then rinse with five changes of methanol with agitation, face up.
- (l) Remove the chip and blow it dry with dry nitrogen boil off; store in a dry box.
- (m) Repeat steps g-l for each chip.

- (n) If long term storage is planned, store the GaAs in an inert atmosphere (ie., in a dry box flushed with dry  $N_2$ ) following the procedure outlined by Schwartz in the attached paper.

Notes for the anodization steps.

- Shape the platinum wire used as a cathode for the anodization in the form of a 1" diameter loop with a "tail" in the plane of the loop having a hook at its end; The "tail" and hook should be fashioned so that they will hold the loop fully immersed in the anodizing solution.
- Be sure to change the chemicals for each crystal. Prepare all items beforehand.

# The Anodization of GaAs and GaP in Aqueous Solutions

## Appendix A:

B. Schwartz,\* F. Ermanis, and M. H. Brastad

Bell Laboratories, Murray Hill, New Jersey 07974

### ABSTRACT

The anodic oxidation of GaAs and GaP in properly conductivity- and/or pH-adjusted water has been successfully demonstrated under both constant voltage and constant current conditions. With  $H_3PO_4$  as the acidic conductivity/pH modifier, uniform, well-controlled oxides have been grown in the pH range 2.5-3.5. The oxide thickness-voltage relationships for both GaAs and GaP are linear, with slopes of approximately 20 and 12 Å/V, respectively. At room temperature, oxides as thick as 3600 and 2000 Å can reproducibly be grown on GaAs and GaP, respectively; at 100°C, an oxide as thick as 5000 Å has been grown on GaAs. Under basic conditions, with  $NH_4OH$  as the conductivity/pH modifier, oxides have been grown in the pH range of 10-11, but dissolution of the oxide in the bath results in much poorer control than in the acidic system; this dissolution effect can be utilized more in the line of electroetching than in simple oxide formation. Anodic oxidation, with relatively little oxide dissolution, has also been accomplished in near neutral-pH water (i.e., ~7) with  $(NH_4)_2HPO_4$  as the conductivity/pH modifier. Restricted-area oxidation and/or etching has been demonstrated whereby a pre-fabricated photoresist pattern is used to define restricted areas for anodization; lines as narrow as 5  $\mu$  wide are readily delineated. Anodization in aqueous solutions containing either  $Cl^-$  or  $NO_3^-$  ions is shown to result in simple electroetching, and current densities in the range 10-20 mA/cm<sup>2</sup> are demonstrated to be most effective for controlled electroetching. The grown oxides are soluble in HCl,  $HNO_3$ , and  $H_2SO_4$ , and are affected by prolonged contact with water. If properly baked, however, the oxide grown on GaAs shows no evidence of change in months of storage in laboratory air; the oxide grown on GaP does show evidence of moisture absorption after 1 month of equivalent storage. A preliminary analysis of some of the controlling electrical factors during anodization shows that under constant voltage conditions, the current ( $I$ ) varies as

$$I = \sqrt{\frac{A}{Bt + C}}$$

and under constant current conditions, the time derivative of the voltage is a constant.

The growth of native oxides on GaAs and GaP by galvanic and anodic techniques (1-4) using 30% aqueous solutions of  $H_2O_2$  as the electrolyte has been shown to be a useful new technology for passivation of semiconductor device surfaces (5, 6), as a diffusion mask (7), and for selective area etching (2). The use of a buffered aqueous solution for the growth of an anodic oxide on GaP has recently been described (8). This paper describes the successful results of growing anodic oxides on GaAs and GaP using water as the electrolyte, under the proper conductivity and/or pH conditions. For both materials, the oxide thicknesses are approximately linear with applied voltage, but the complication of rapid film dissolution at the oxide-electrolyte interface can be an appreciable correction factor to be considered. In fact, it is shown that the entire range, from anodic oxidation with minimal oxide etching to total anodic etching with minimal residual surface oxide, can be controllably achieved by proper choice of anion, pH, and conductivity control. The choice of anion in the pH/conductivity modifier can be a very important factor, and conditions where simple anodic etching is achieved are described.

Finally, the feasibility of combining photoresist technology and oxidation in water to make restricted area oxide patterns directly on the surface of the semiconductor are shown; under the proper solution conditions, electrolytic etching through these photoresist masks can also be accomplished readily.

\* Electrochemical Society Active Member.

Key words: native oxides, compound semiconductors, anodic oxidation.

### Experimental Procedure

The electrolytic cell used for this study was almost identical to that previously described (1), except that either a constant voltage or a constant current supply could be used as the power source. Because the reagent was water instead of  $H_2O_2$ , the lack of reaction between the platinum cathode and the electrolyte eliminated the need for a baffle in the system, and a simple quartz beaker was, therefore, used as the bath container. The semiconductor samples were either partly or fully immersed in the bath while held in an aluminum clamp since the aluminum also anodized in water (3). The water used in these studies was 15 megohm-cm at the resin bed and 6 megohm-cm at the point of use; the pH of the starting water was approximately 6.5. When anodization was attempted in this water directly, it was found that the conductivity was so low that almost the entire voltage drop occurred across the solution (2) and very little appeared at the semiconductor-electrolyte interface, so that no oxide growth was achieved. The pH of the water was adjusted downward with  $H_3PO_4$  or upward with  $NH_4OH$ ; in one series of anodizations, the pH was made nearly neutral (i.e., 7.8) with  $(NH_4)_2HPO_4$  as the conductivity modifier.

The GaAs slices were all n-type, (100)-oriented, Si- or Te-doped at about  $1 \times 10^{18}$ /cm<sup>3</sup>. Most of the GaP used was n-type, (111)-oriented, Se-doped with  $|N_D - N_A|$  between 0.1 and  $1 \times 10^{18}$ . A few experiments were performed on p-type, Zn-doped GaP with  $|N_A - N_D| = 0.5$  to  $5 \times 10^{18}$ . All samples were chem-

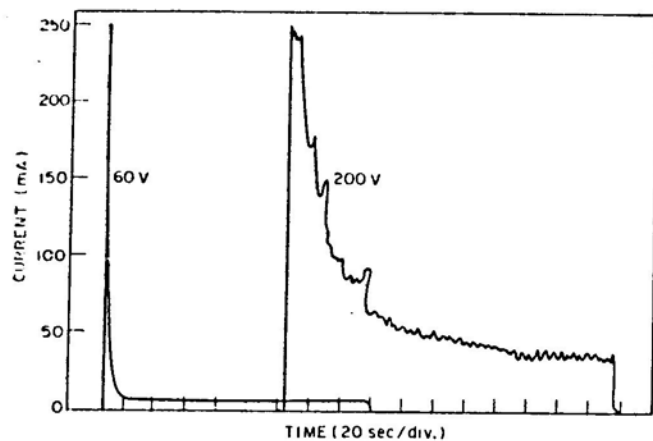


Fig. 1. Current vs. time during anodization of n-type GaAs at constant voltage of 60 and 200V in acidic ( $\text{pH} = 2.5$ ) water.

mechanically polished directly from the saw-cut condition in a 0.075% bromine-in-methanol solution, on a PAN-W polishing cloth. Following this step, the slices were given at least 12 cycles of acetone wash in a Soxhlet extractor, then air dried and stored until used.

After anodization, the samples were either water-rinsed and air-dried, or water-rinsed and bake-dried in a nitrogen-purged oven for 1 hr at  $95^\circ\text{C}$  and 2 hr at  $250^\circ\text{C}$ ; then the thickness and index of refraction were determined on a Rudolph ellipsometer<sup>1</sup> at 6328Å radiation.

### Experimental Results

**Anodic oxidation in acidic [ $\text{H}_3\text{PO}_4$ ] water: GaAs.**—A monitoring of the current as a function of time, for constant voltage anodizations and with the room temperature water adjusted to a pH of 2.5, yielded the data presented in Fig. 1. At voltages up to and including 170V, all of the results appeared similar to the 60V curve; the entire surface area of the grown film was uniform in color and specular. However, at biases in the range 180–200V, the data shown as the 200V  $I-t$  curve resulted. The films were still uniform in color, but were slightly hazy in appearance; above 200V, the samples took on a nonuniform mottled look (1).

A monitoring of the voltage as a function of time, for constant current anodization, with the room temperature water adjusted to a pH of 2.5, yielded the data shown in Fig. 2.<sup>2</sup> The conclusions to be drawn from these data are: (i) the apparent critical current density necessary to start the oxide growth, and (ii) the apparent linear relationship between voltage and time, which is to be compared with the very nonlinear current-time curve determined for constant voltage anodization (see Fig. 1). In the case of constant voltage, if the anodization is allowed to proceed long enough for the asymptotic current level to be approached, or in the case of constant current a predetermined voltage level is reached,<sup>3</sup> a plot of the resulting oxide thickness against applied voltage yields a straight line, as shown in Fig. 3. Note that this curve extrapolates back through the origin and has a slope of about 20 Å/V.

In order that the influence of temperature on the thickness-voltage curve might be determined, a series of samples were anodized in water at  $100^\circ\text{C}$  (i.e., the water was adjusted to a pH of 2.5 at room temperature and then brought to its boiling point). The data obtained are shown in Fig. 4; note that the lower por-

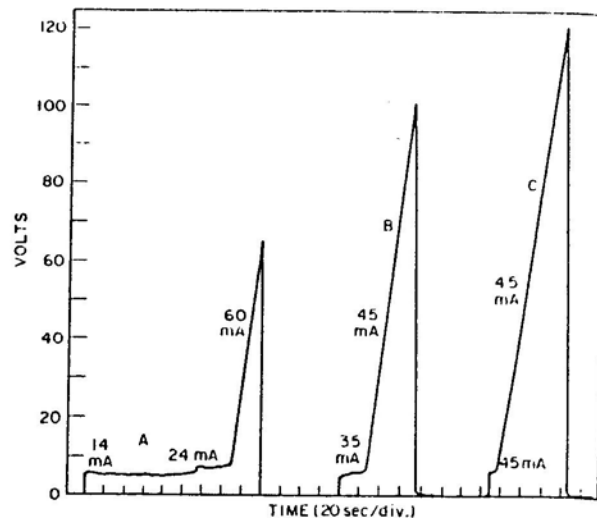


Fig. 2. Voltage vs. time during anodization of n-type GaAs in the constant current mode in acidic ( $\text{pH} = 2.5$ ) water.

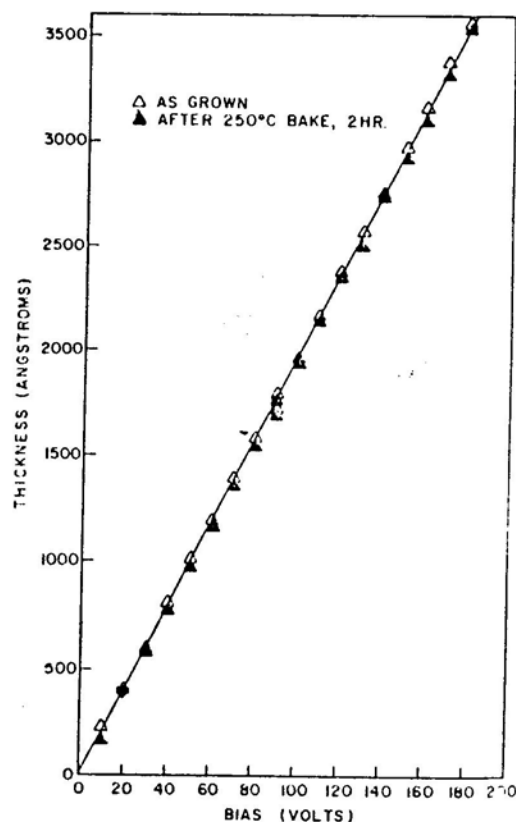


Fig. 3. Oxide thickness vs. bias voltage for n-type GaAs anodized at constant voltage in acidic ( $\text{pH} = 2.6$ ) water.

tion of this curve is linear with a slope of approximately 25 Å/V, but that as the voltage increases the thickness dependence rises superlinearly, approaching almost 50 Å/V at the upper end before the "limiting" voltage is reached. This higher order dependence is similar to that observed in the anodization of GaAs in boiling  $\text{H}_2\text{O}_2$  (3).

The effect of varying the pH on the growth of an oxide at a fixed bias (i.e., 45V) is shown in Fig. 5; note the falloff in growth rate below a pH of 2.5 and above a pH of 3.5.

As was observed in the anodization of GaAs in  $\text{H}_2\text{O}_2$  (3), a bake in dry nitrogen at about  $250^\circ\text{C}$  has been found suitable for stabilizing the grown oxide. Thickness changes of less than 10% and refractive index shifts (i.e., from  $n = 1.80$ ) of less than  $\pm 0.01$  have been observed during this drying procedure. The stabilized oxide has been found to be soluble

<sup>1</sup> A few measurements were also made on a Gaertner ellipsometer with 5461Å light.

<sup>2</sup> Although the area of the exposed surfaces was held relatively constant at about  $1\text{ cm}^2$ , there was enough unmeasured variation to indicate that the currents listed do not necessarily reflect the absolute current densities.

<sup>3</sup> Assuming the time to be long enough for the achievement of a steady-state condition, and the voltage to be near neither the breakdown limit of the oxide nor the saturation limit of the power

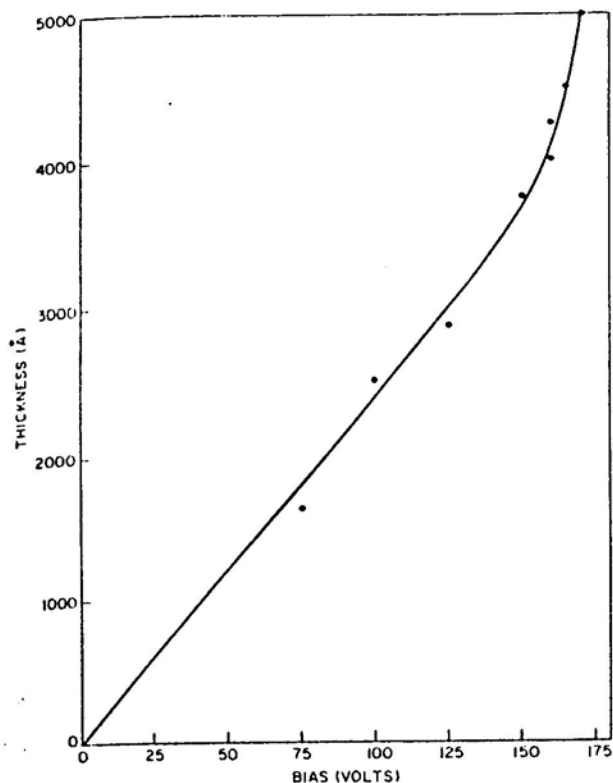


Fig. 4. Oxide thickness vs. bias voltage for n-type GaAs anodized at constant voltage in acidic ( $\text{pH} = 2.6$ ) water at  $100^\circ\text{C}$ .

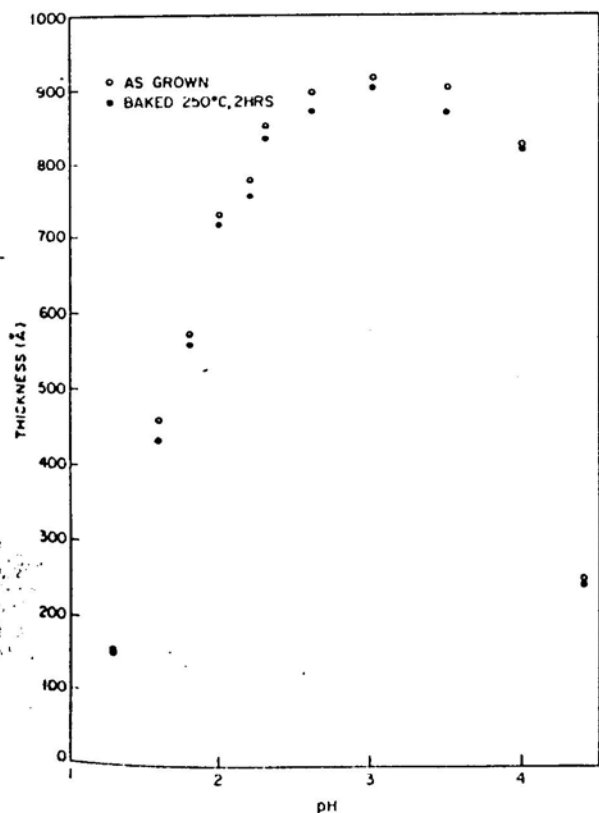


Fig. 5. Variation of oxide thickness as a function of  $\text{pH}$  for n-type GaAs anodized at constant 45V.

aqueous solutions of  $\text{NH}_4\text{OH}$  and  $\text{HCl}$ , both in the concentrated forms (15 and 12M, respectively) and diluted 10 parts water to 1 part concentrated base or acid. Again, as was found with the anodic oxide grown in  $\text{H}_2\text{O}_2$ , the oxide grown in water was insoluble in  $\text{Br}_2\text{-CH}_3\text{OH}$  whether it was baked or not. Exposed to room air, the baked oxides showed no ob-

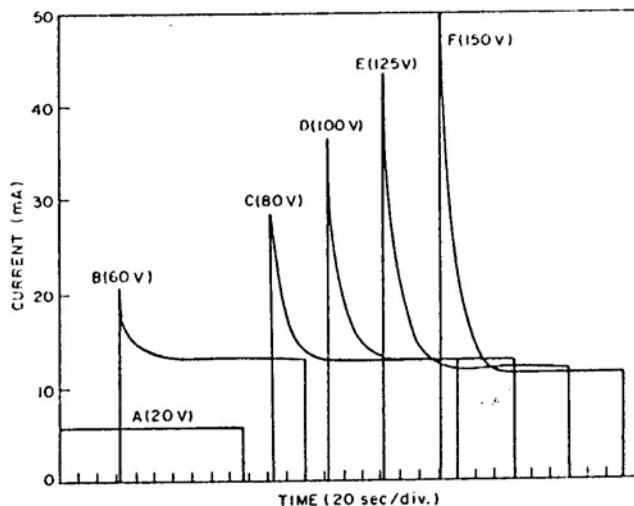


Fig. 6. Current vs. anodization time for n-type GaAs in basic water ( $\text{pH} = 10$ ) at constant voltage.

servable changes over a period of 10 months. In direct contact with deionized water, however, both the as-grown and the baked oxides developed localized pin-hole-type defects and nonuniform thickness changes.

Optically levered laser-beam measurements (9) on 10 mil thick GaAs slices anodized in acidic water indicated that there is no measurable stress<sup>4</sup> induced in the samples after anodization, after baking at  $250^\circ\text{C}$ , or after annealing at  $650^\circ\text{C}$  in dry nitrogen for  $\frac{1}{2}$  hr.

**Anodic oxidation in basic  $[\text{NH}_4\text{OH}]$  water: GaAs.**—Figure 6 shows the results of attempting anodization of GaAs, in room temperature water adjusted to a  $\text{pH}$  of 10, under various constant voltage conditions. The most obvious result is that at 20V no oxide of any appreciable thickness grew and no etching was achieved. Secondly, even where oxide growth was evident (i.e., by current falloff with time), the ultimate leakage current was relatively high (i.e., 2 to 3 times as high as in the acidic case shown in Fig. 1), again indicating rapid dissolution of the oxide under steady-state conditions. Further evidence for this rapid dissolution of the native oxide in basic water is shown in Fig. 7. In this case, an initial bias of 120V was applied to the sample for 40 sec, after which time the voltage was dropped to only 20V; this lower bias was then maintained for approximately 60 sec. The sequence was then repeated twice before the power supply was turned off. On examination of any complete cycle in Fig. 7, it becomes quite obvious that during the second part of the cycle, where the bias on the sample was maintained at the lower voltage (i.e., 20V), the resistance of the cell was changing with time. This resistance change was the result of a thinning of the oxide layer by dissolution, until the very thin, steady-state oxide thickness for the 20V was achieved.

Anodization under constant current conditions in water at a  $\text{pH}$  of about 10 also yielded data indicative of excessive etching of the oxide (see Fig. 8). In addition, whereas constant current anodization in acidic water yielded a linear dependence of the voltage on time, there is evidence that deviation from linearity occurred in a number of cases for the basic system.

The nonreproducibility of oxide thickness for basic-water oxidation was also illustrated when a plot of thickness vs. voltage was attempted; the scatter of the points was so large as to make this kind of plot essentially meaningless, thus indicating the poor control for growing oxides in high  $\text{pH}$  solutions. However, the potential for use of this  $\text{pH}$  range as an electrolytic etching region becomes attractive.

**Anodic oxidation in acidic  $[\text{H}_3\text{PO}_4]$  water: GaP.**—When GaP was anodized in room temperature water

<sup>4</sup> Minimum measurable stress level in GaAs is  $1.2 \times 10^8$  dynes/cm (2).



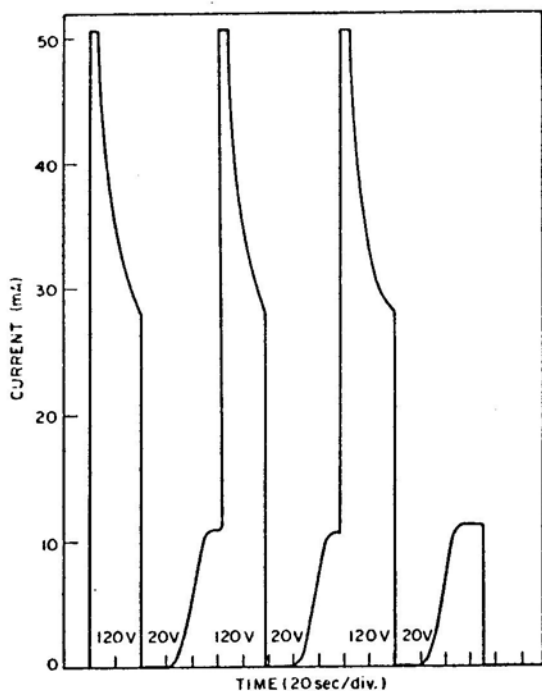


Fig. 7. Behavior of anodization current as a function of time during anodization of n-type GaAs in basic ( $\text{pH} = 11$ ) water at cycled biases of 120 and 20V. The current maximum of 52 mA was due to a current limiter on the powder supply used.

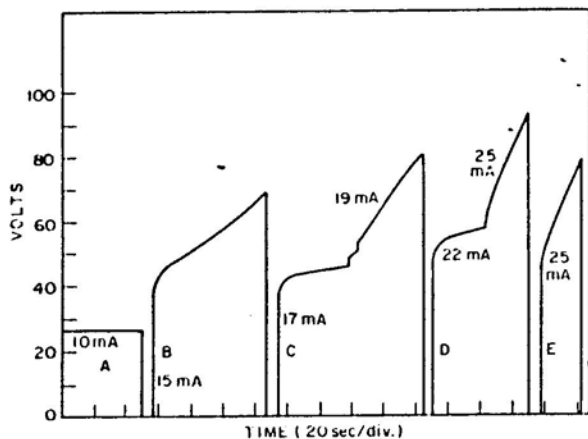


Fig. 8. Voltage vs. time during anodization of n-type GaAs in the constant current mode in basic ( $\text{pH} = 10$ ) water.

adjusted to a pH of 2.8, at either constant voltage or constant current, curves similar to those shown in Fig. 1 and 2 were obtained. Figure 9 is a plot of thickness vs. voltage for both p- and n-type GaP anodized at constant voltage. The plot also shows the negligible effect of drying on the film thickness. The slopes of the straight lines through both sets of data are approximately 12 Å/V. The one for n-type GaP, however, is shifted toward higher voltages, thus showing that n-type material anodized at identical voltages grows an oxide approximately 100 Å thinner than p-type material. This voltage shift is believed to be due to the different (i.e., lower) doping level of the n-type samples (10). In any case, the ultimate oxide thickness achievable in the anodization of GaP is lower than that for GaAs which can be anodized under similar conditions at about 20 Å/V.

Another effect that is delineated in the data of Fig. 9 is the nonlinearity of the apparent film thickness in both the low and the high voltage ranges. A probable reason for the scatter in the low voltage range is the relatively large uncertainty in the assignment of thickness values from the ellipsometrically measured refractive index. In this, the thin film re-

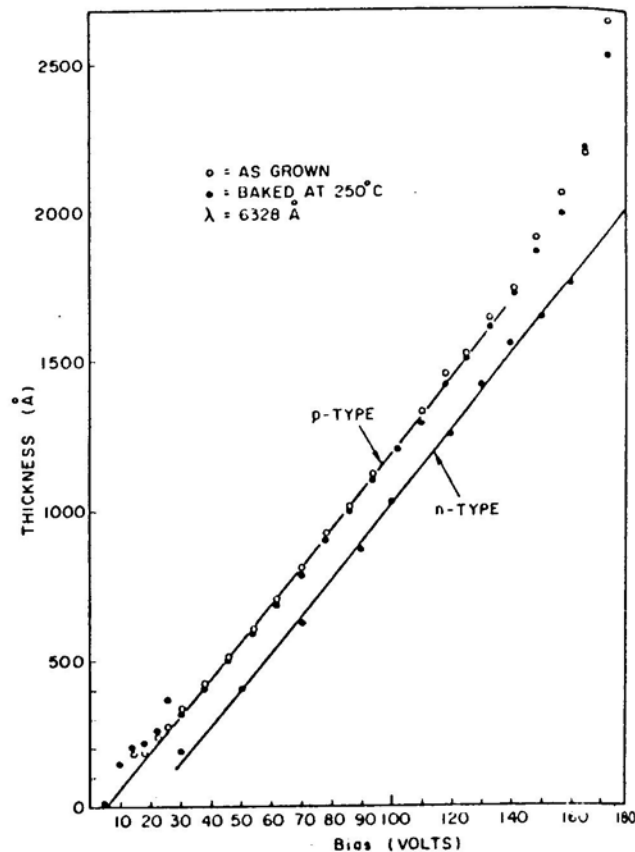


Fig. 9. Ellipsometrically determined oxide thickness vs. applied voltage for p- and n-type GaP anodized in acidic ( $\text{pH} = 2.7$ ) water. The wavelength of the measuring light source was 6328 Å.

gion (11). It is believed that in the thick oxide region of the curve, the deviation from linearity is only an artifact of the measurement; evaluation of the film thickness on a rotating-analyzer ellipsometer (12) yields data to indicate that the thickness extrapolates linearly to about 200V. The fact that the refractive index appears to vary as a function of the oxide-forming voltage (see Fig. 10), and that the variation seems to be measurement wavelength dependent are thought to be due to an anomalous reflectivity effect at the oxide-semiconductor interface (4). An attempt is under way at this time to achieve an understanding of this anomaly.

When the effect of pH on the growth of the GaP-oxides in acidic media was examined, the data shown in Fig. 11 were obtained. Again, a falloff in oxide thickness was observed below a pH of about 2 and above about 3.5. As noted in Fig. 9, baking the oxidized samples at 250°C for 2 hr in a nitrogen-purged oven had very little effect on the oxide thickness. However, anodization at a pH less than 2 yielded some very startling results in the aging characteristics of the formed oxide. Whereas an oxide grown on GaP at pH = 2.7 and not stabilized can sit in a flat-pack on the shelf for about 2 weeks with no apparent change in thickness or refractive index, a film grown at a pH of 1.9 or less will show drastic color changes when allowed to sit unstabilized for less than 1 day under identical conditions. The instability of the oxide becomes evident on the baked samples as well after storage of about 1 month, when localized color changes can be observed. The new color spots are those of oxides thicker than those originally grown, thus indicating a swelling of the oxide, possibly due to absorption of moisture from the atmosphere. This relative instability is to be compared to the case of a galvanic oxide grown on GaP which was bake-dried and showed no change in thickness or refractive index after storage in room air for 2.5 years.

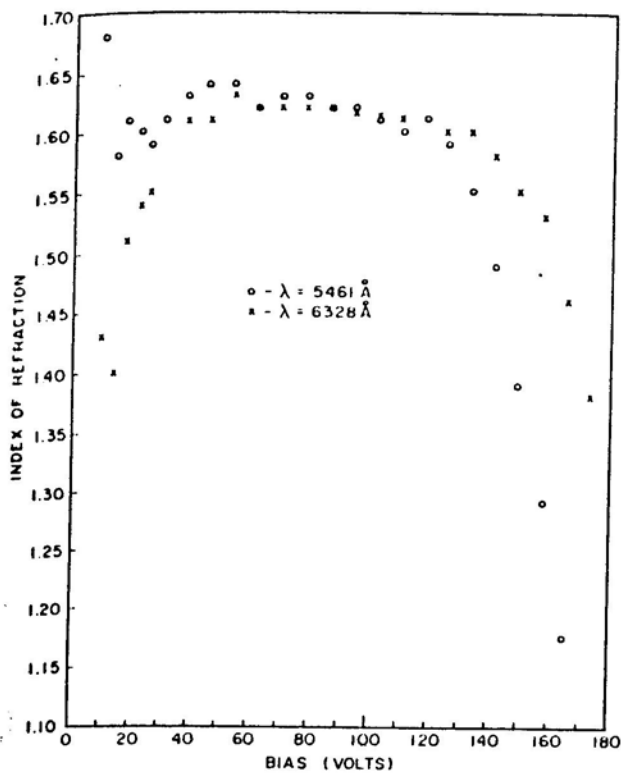


Fig. 10. Index of refraction of GaP-oxide films as a function of anodization voltage, in acidic ( $\text{pH} = 2.8$ ) water determined ellipsometrically on the same sample with 2 different wavelengths of light:  $5401 \text{ \AA}$  (○) and  $6328 \text{ \AA}$  (×).

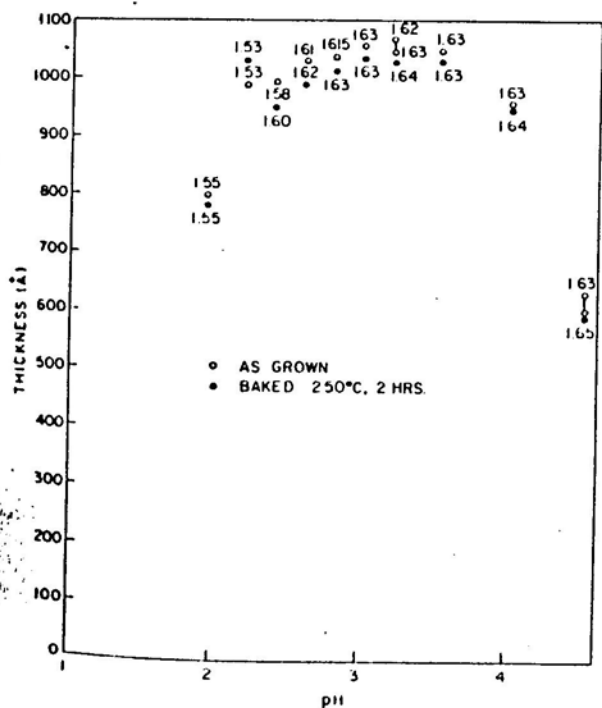


Fig. 11. Thickness of GaP-oxide films grown at a constant bias of 100V, as a function of the pH of the acidified water electrolyte. The figures near the symbols denote the index of refraction before (○) and after (●) a 2 hr,  $250^\circ\text{C}$  bake.

In order that the effects of water on anodized and baked GaP might be observed, 2 samples with oxides 750 and 2000 Å thick were immersed in deionized water for a period of 4 weeks. After an initial loss of about 20 Å during the first 2 or 3 days, the sample remained covered with an oxide which showed a tendency toward increasing thickness. Owing to its nonuniform

appearance, however, no exact thickness measurements were obtainable.

**Anodic oxidation in basic  $[\text{NH}_4\text{OH}]$  water: GaP.**—As was found with GaAs, anodization of GaP in water at pH of 10-11 can yield relatively thick surface oxides as an end product. However, again as with GaAs, the high solubility of the oxide in the high pH electrolyte causes large errors when attempts are made to reproduce an oxide thickness-voltage plot (i.e., very short delays in removing the sample from the solution and rinsing it can introduce large errors due to the severe etching of the formed oxide). It is therefore recommended that this pH range be considered more for its electroetching potential than for its oxide growth capability.

**Anodic oxidation in near neutral  $[(\text{NH}_4)_2\text{HPO}_4]$  water: GaAs.**—Because deionized water (i.e., 16 megohm-cm) has extremely low conductivity, it is very difficult to achieve an anodization of GaAs or GaP at moderate voltages. It was therefore decided to attempt to modify the conductivity of the deionized water without going very far in either the acidic or the basic direction. This is easily accomplished by the use of the ammonium acid phosphate salts, and we chose to examine  $(\text{NH}_4)_2\text{HPO}_4$  as the additive; a 0.1N aqueous solution of this reagent will automatically adjust to a pH of 7.8. When a constant voltage anodization at 100V was attempted, the classic rapid current falloff was observed and a gold-colored oxide (i.e., 2000 Å) was found on the sample. Adjusting the pH of the solution to 7.15 by the addition of  $\text{H}_3\text{PO}_4$  also yielded good oxidation. It appeared that some slight etching of the oxide occurred in the original pH 7.8 solution, and less in the 7.15 pH solution. A further discussion of the potential of this system appears in the next section which deals with masked anodization.

**Restricted-area anodic oxidation: GaAs and GaP.**—All anodizations described thus far were performed by immersing the samples in the electrolyte and anodizing the entire exposed surface area. Subsequent to anodization photolithographic-processing has been utilized to define specifically required oxidized and nonoxidized regions of the surface for further device fabrication needs (13). Thus certain implied restrictions were placed on the condition of the sample to allow for this processing approach (e.g., no nonoxidizable ohmic contacts were to be exposed). In addition, it had been noted (13) that in the development of the photoresist (i.e., AZ-111) the developing solution was caustic enough that both the exposed photoresist and the underlying grown oxide were removed simultaneously. Although this single develop-etch process simplifies the operation of oxide pattern generation, it provides for a less controlled geometry in that undercutting of the oxide is a severe problem when one attempts to achieve fine line definition. When a negative resist was used with a nonalkaline developer, the single develop-etch step was eliminated. However, it was difficult to control the amount of oxide undercutting during the oxide etch step.

As an alternative to using oxidation first and then photolithography, an experiment in reversing the order (i.e., first photolithography and then anodization) was attempted. When this was performed in the 30%  $\text{H}_2\text{O}_2$  electrolytic system, it was found that the photoresist could survive only for seconds because of the strong oxidizing action of the  $\text{H}_2\text{O}_2$  on the organic polymer. However, when the same experiment was tried on some n-type GaAs in acidic water ( $\text{pH} = 2.05$ , 55V bias, 60 sec anodization time) with the Ealing test pattern as the geometry system, localized oxidation was observed. The sample was then placed in an acetone-containing Soxhlet extractor (after being blot-dried but not baked) and the photoresist was stripped from the sample. Subsequent baking in a nitrogen-purged oven at  $95^\circ\text{C}$  for 1 hr and then at  $250^\circ\text{C}$  for 2 hr yielded the sample shown in Fig. 12 (i.e., the dark

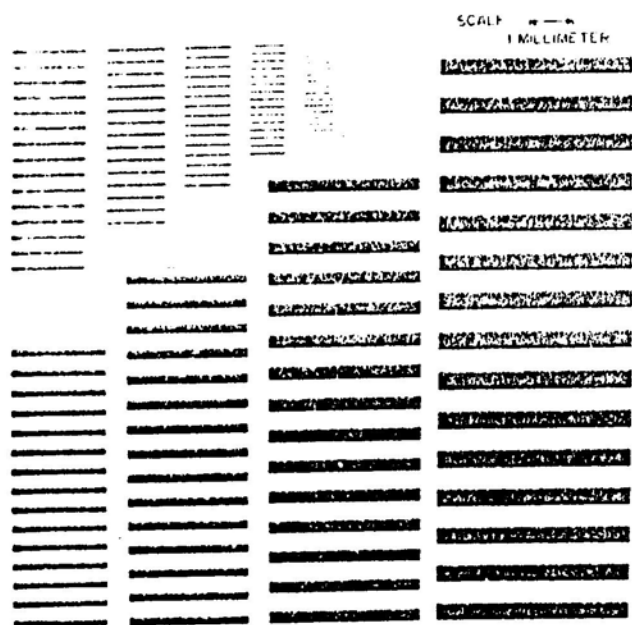


Fig. 12. A GaAs sample with deposited Ealing test pattern after anodization at 55V in water of pH = 2.5 and after removal of the photoresist. The oxidized areas are dark; original magnification was approximately 30X.

regions are the oxidized areas). On careful examination of the generated oxide pattern, it was determined that oxide stripes  $5\mu$  wide were well delineated on the surface of the GaAs.

When a similar experiment was attempted in basic water (i.e., pH = 10,  $\text{NH}_4\text{OH}$ ), similar oxidation results were obtained. However, when the sample was allowed to sit in the electrolyte after the voltage was turned off, the oxide redissolved. A restricted-area etching experiment was then performed whereby a photoresisted sample was anodized in basic water under conditions similar to those shown in Fig. 7; 120V for 40 sec and then 20V for 60 sec for a total of 3 complete cycles. Subsequent Talystep scanning of the sample surface (after removal of the AZ-111 with acetone) showed that the 3 cycles of oxidation and dissolution produced steps about  $6000\text{\AA}$  deep. The delineation of the Ealing pattern was only fair, however, because the AZ-111 had obviously been attacked by the alkaline water.

In either case (i.e., acidic or basic water), after a few minutes exposure of the photoresist to the electrolytic solution, deterioration of the resist was observed. However, when a similar experiment was performed in water with  $(\text{NH}_4)_2\text{HPO}_4$  as the conductivity modifier, oxidation was observed; and negligible attack occurred on the photoresist even after 10 min exposure.

**Anodic etching: GaAs and GaP.**—Up to this point, the discussion has centered about the anodization of GaAs and GaP in phosphate or hydroxide solutions. Previous observations revealed that a change in the anion used for pH modification to  $\text{NO}_3^-$  or  $\text{Cl}^-$  resulted in severe inhibition of oxide growth (2). A more detailed examination of this effect indicates that electrolytic etching takes place in the presence of these two anions (i.e., the oxide never really grows very thick before it is dissolved in the electrolyte). The contamination level required before an anion will cause the system to shift from oxide growth to etching has been determined. The approach used was to take concentrated HCl and  $\text{HNO}_3$  and dilute, 1 ml acid to 99 ml water. One drop of this diluted acid<sup>5</sup> was then added each time to about 400 ml of  $\text{H}_3\text{PO}_4$ -acidified water preset at a pH of 3. An anodization

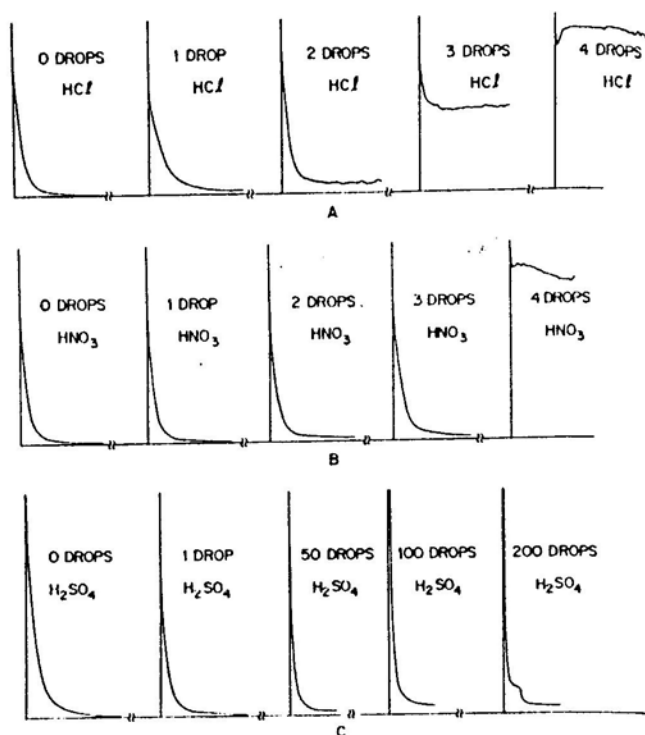


Fig. 13. Current-time curves for a constant voltage (50V) anodization of n-type ( $N_D - N_A \approx 1 \times 10^{18} \text{ cm}^{-2}$ ) GaAs in acidic (pH = 3) water. (A) Contamination with dilute HCl where each drop of additive provided  $4.4 \times 10^{-6}$  moles of HCl. (B) Contaminated with dilute  $\text{HNO}_3$  where each drop of additive provided  $6.2 \times 10^{-6}$  moles of  $\text{HNO}_3$ . (C) Contaminated with dilute  $\text{H}_2\text{SO}_4$  where each drop of additive provided  $6.8 \times 10^{-6}$  moles of  $\text{H}_2\text{SO}_4$ .

curve (constant voltage) was then generated using a new piece of standard n-type, silicon-doped GaAs with  $N_D - N_A \approx 1 \times 10^{18}$ , at a fixed 50V bias. Figure 13 A and B are the current-time curves of the samples after zero to four drops of diluted acid were added to the electrolytic solution. Note, in Fig. 13A, that there was a very gradual increase in the saturation current for the HCl-contaminated solution from almost the first drop, but that there was a large shift on the addition of the third and fourth drops of contaminant. The  $\text{HNO}_3$ -contaminated system did not appear to respond until at least the third drop, but by the fourth drop it reacted severely. Considering that one drop of added dilute solution caused an impurity level of about 0.2-0.3 parts per million, it appears that at approximately one part per million of either  $\text{NO}_3^-$  or  $\text{Cl}^-$  radical effects are observed.

Because not all acidic anions are deleterious to oxide growth (e.g., phosphate, tartrate, citrate), it was decided to examine  $\text{H}_2\text{SO}_4$  to determine the effect of the sulfate anion. Figure 13C shows that very little effect on the anodization curves was observed up to about 100 drops of diluted  $\text{H}_2\text{SO}_4$  and that at 200 drops, a moderate effect was beginning to emerge. Clearly, the system can tolerate almost two orders of magnitude more sulfate ion than it can either chloride or nitrate ion.

Going one step further, the conditions for straightforward electrolytic etching of GaAs and GaP in dilute solutions of HCl and  $\text{HNO}_3$  have been studied. Table I is a summary of the etching characteristics of both GaAs and GaP in these reagents as a function of acid concentrations and current densities. An analysis of these data combined with impressions obtained on visual examination of the surface after etching can be summarized as follows: (i) A current density of  $40 \text{ mA/cm}^2$  and above "pulverizes" the surface, leaving a black-appearing residue on the surface. (ii) A current

Table I.

Run number	Acid	Sample*	Concentration (normality)	Sample surface area (cm <sup>2</sup> )	Orientation	Current** (mA)	Voltage (V)	Amount removed (Å)	Electron conversion efficiency (%)
1	HNO <sub>3</sub>	GaAs	1	0.5	(100)	5.0	1.6	3,750	12.5
2	HNO <sub>3</sub>	GaAs	1	0.5	(100)	10.0	2.5	5,000	8.3
3	HNO <sub>3</sub>	GaAs	1	0.5	(100)	50.0	2.3	100,000	—
4	HNO <sub>3</sub>	GaAs	1	0.5	(100)	1.0	1.2	750	—
5	HNO <sub>3</sub>	GaAs	0.1	0.5	(100)	5.0	2.4	6,000	20.6
6	HNO <sub>3</sub>	GaAs	0.1	0.5	(100)	10.0	3.2	7,125	13.8
7	HNO <sub>3</sub>	GaAs	0.1	0.5	(100)	20.0	3.4	64,000	—
8	HNO <sub>3</sub>	GaAs	0.1	0.5	(100)	1.0	1.0	2,000	—
9	HNO <sub>3</sub>	GaAs	0.01	0.4	(100)	5.0	3.8	675	1.7
10	HNO <sub>3</sub>	GaAs	0.01	0.4	(100)	10.0	6.2	1,300	1.6
11	HNO <sub>3</sub>	GaAs	0.01	0.4	(100)	1.0	2.0	750	9.5
12	HCl	GaAs	0.1	0.5	(100)	1.0	1.0	700	11.0
13	HCl	GaAs	0.1	0.5	(100)	5.0	2.0	10,000	33.3
14	HNO <sub>3</sub>	GaP	0.1	0.5	(111)	5.0	—	80	—
15	HNO <sub>3</sub>	GaP	0.1	0.5	(111)	10.0	—	1,250	—

\* All samples were n-type.

\*\* All samples anodized for 300 sec.

delineating some of the residual polishing scratches. (iii) The most efficient current density for good electrolytic etching is between 10 and 20 mA/cm<sup>2</sup>.

### Discussion

**Analysis of electrical control parameters.**—Until this point only the phenomenological observations made during the anodization of GaAs and GaP have been described. In this section an attempt is made to obtain better understanding of the anodization processes by developing a set of current-voltage-time equations based on a very simple linearized equivalent circuit, shown in Fig. 14. In this circuit the oxide resistance is represented by a variable resistance,  $\tau$ , which during anodic oxidation varies from essentially zero to extremely large values while during anodic etching remains very small.

From the two basic equations:

Ohm's law

$$V = I(\tau + R) \quad [1]$$

where  $\tau$  and  $R$  are the resistances of the oxide and of the solution, respectively, and

Faraday's law

$$\tau = K \int_0^t I(t) dt \quad [2]$$

where the constant  $K$  includes all parameters assumed to be constant, such as the geometrical factors, the oxide composition, resistivity, and electron-to-oxide conversion efficiency, etc. The time-dependent form of Ohm's law which results is

$$\frac{\partial V}{\partial t} = \left( R + K \int_0^t I(t) dt \right) \frac{\partial I}{\partial t} + KI^2 \quad [3]$$

For the case of constant current,  $I = I_a$ , the solution of

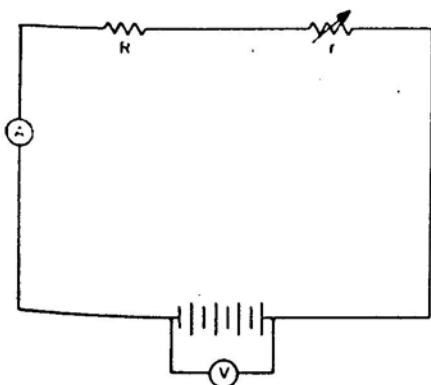


Fig. 14. Simplified circuit diagram of the anodizing system:  $R$ , resistance of the electrolyte;  $r$ , resistance of the oxide layer;  $V$ , applied bias;  $I$ , current following.

Eq. [3] is

$$V = KI_a^2 t + I_a R \quad [4]$$

For the case of constant voltage,  $V = V_a$ , Eq. [3] reduces to

$$(\tau + R) \frac{\partial I}{\partial t} + KI^2 = 0 \quad [5]$$

which has a solution

$$I = \sqrt{\frac{V_a^2}{R^2 + 2V_a K t}} \quad [6]$$

or with proper substitutions

$$\tau = \sqrt{R^2 + 2V_a K t} - R \quad [7]$$

The voltage drop across the oxide,  $V_o$ , is then

$$V_o = V_a \left( 1 - \frac{R}{\tau + R} \right) \quad [8]$$

One can now readily see, that by taking the derivative of Eq. [4], the time variation of voltage at constant current is a constant, which is exactly what was observed in the data of Fig. 2. Since in this analysis it was assumed that the resistivity, among other factors, was held constant in order to yield the linear voltage-time dependence, the experimental verification of this linear dependence implies that the resistivity of the growing film is constant under the constant-current anodization conditions studied here.

Also note, from Eq. [6], that the current-time relationship, at constant voltage, is a relatively complicated expression. Whereas previously an exponential dependence of current on time had been assumed (2), one can now see that an inverse square root form of dependence on time could be governing the situation. The extremely rapid current falloff in the initial stages of anodization is now recognized to be due to the operation of the parameter  $K$  (which has a value of about  $10^5$  ohms-coulombs<sup>-1</sup>) on  $t$  in Eq. [6].

In utilizing the equivalent circuit shown in Fig. 14, the situation has been drastically oversimplified. The assumption is made for example, that  $R$  is a simple constant, that there is no voltage drop in the semiconductor, and that there is no charge storage in the oxide. These simplifications have allowed a working basis from which to start. These corrections may now be incorporated into the equations just developed.

Since the simple properties of concentrated acids and bases are well known (15), one can easily determine that the reagent concentrations for the anodic oxidation systems under study are approximately 0.002M for H<sub>3</sub>PO<sub>4</sub> and 0.02M for NH<sub>4</sub>OH. In Tables II and III are listed the resistivity, equivalent conductance, and pH as functions of molarity of H<sub>3</sub>PO<sub>4</sub> and NH<sub>4</sub>OH solutions, respectively (only values up to about 10M are listed). On the basis of these data, one might

Table II.

Concentration (equiv./liter)	Resistivity* (ohm-cm)	Equivalent (19, 20) conductance (mho-cm <sup>2</sup> /g-equiv.)	pH (21, 15)
Pure water	$2.5 \times 10^7$	—	7
0.0 (infinite dilution)	—	376	—
0.002 (H <sub>3</sub> PO <sub>4</sub> )	0.64	311.9	—
0.01	4.50	222.0	~2.15
0.05	37.71	132.0	—
0.1	96.15	104.0	1.5
0.43	71.44	32.55	—
0.89	39.48	28.46	—
1.66	23.55	25.57	—
5.37	12.40	15.01	—
7.96	9.98	12.59	—
11.20	7.80	11.44	—

\* Calculated.

Table III.

Concentration (equiv./liter)	Resistivity* (ohm-cm)	Equivalent (22) conductance (mho-cm <sup>2</sup> /g-equiv.)	pH (14)
Pure water	$2.5 \times 10^7$	—	7
0.0 (infinite dilution)	—	242	—
0.0001 (NH <sub>4</sub> OH)	$15.2 \times 10^4$	(66)**	—
0.0005	$52.6 \times 10^4$	38	—
0.001	$35.7 \times 10^4$	28	—
0.005	$15.2 \times 10^4$	13.2	10.6
0.01	$10.4 \times 10^4$	9.6	—
0.05	$43.5 \times 10^2$	4.6	—
0.1	$30.3 \times 10^2$	3.3	11.1
0.5	$14.8 \times 10^2$	1.35	—
1.0	$11.2 \times 10^2$	0.89	11.6
5.0	$9.9 \times 10^2$	0.202	—
10.0	$18.5 \times 10^2$	0.054	—

\* Calculated.

\*\* Estimated.

postulate that: (i) The simple solution resistance for the caustic system should be about 5 orders of magnitude higher than for the acid system used, and (ii) because the minimum in the acid system resistivity is close to the  $2 \times 10^{-3}M$  determined for the electrolyte concentration used, this should be the governing factor in the shape of Fig. 5.

Unfortunately, the data indicate a factor of only about 10 difference in our anode-to-cathode electrical resistance (i.e., approximately 30-3 kohms for base and acid, respectively) and not the factor of  $10^5$  predicted. This higher resistance in the caustic system could also be involved in the very rapid voltage increases noted in Fig. 8. Note that whereas Table II predicts a factor of 20 increase in resistance between pH = 2.15 and 1.5, the data in Fig. 5 show that there is a drop in ultimate thickness of about a factor of 3. Unquestionably, the resistance of the solution is an important factor in the control of oxide formation, but it is not the total answer.

Examining the question of field distribution in going from the solution into the solid anode, one finds that at least five "resistances" must be taken into account: the depletion region at the liquid-oxide interface, the oxide itself, the depletion width in the semiconductor, the resistance in the bulk of the semiconductor, and the contact resistance between the semiconductor and the aluminum-tipped tweezers. One can dispense with the bulk and contact resistances by assuming that they are constant and can be included in  $R$  of Fig. 14. It must be kept in mind, however, that a large change in the free carrier concentration in the semiconductor could introduce an appreciable amount of bulk series resistance, thereby altering the field distribution available for oxidation at the surface. For this reason one should expect moderate effects on the position of the thickness-voltage curve (such as that shown in Fig. 9) for samples with lower or higher free

carrier density than was used to generate any of the voltage thickness curves in this paper.

The three remaining resistances to be considered are the two depletion regions at the liquid-oxide and oxide-semiconductor interfaces and the oxide resistance itself. It was shown recently (16) that when an n-type electrode is used as the anode in either of these electrolytes, a reverse biased Schottky diode situation is achieved. One can therefore expect that the additional voltage drop across the depletion layer in the semiconductor will also cause variation in the position of voltage vs. thickness plots as the doping density of the semiconductor varies. Therefore, in order to be more thorough, one would have to account for this additional voltage drop ( $V_b$ ) in Eq. [8] by subtracting it from  $V_a$  thus

$$V_o(t) = (V_a - V_b)(\tau(t)) \quad [9]$$

One possible way to minimize this doping level effect is to generate free carriers optically, with high intensity light of the proper energy.

Similarly, if one examines the solutions being used for these oxidations one finds that there are  $1.1 \times 10^{18}$  and  $5 \times 10^{17}$  ionized molecules/cm<sup>3</sup> for the H<sub>3</sub>PO<sub>4</sub> and NH<sub>4</sub>OH solutions, respectively. Again, depletion regions are formed on the solution side of the electrolyte-oxide interface because of the higher dielectric constant of water [80 for pure H<sub>2</sub>O as against 11 and 10 for GaAs and GaP, respectively (15, 17)]. Also, the caustic solution will have a larger voltage drop than the acid solution because of the lower free charge density in the former solution. Consideration of the voltage drop,  $V_s$ , across the depletion region on the electrolyte side of the solution-oxide interface results in an additional modification to Eq. [8] shown as

$$V_o = (V_a - V_b - V_s)(\tau(t)) \quad [10]$$

Earlier in this section we concluded that the resistivity of the oxide was a constant because of the linearity of the voltage-time plot of Fig. 2. This does not necessarily mean, however, that the oxide is absolutely uniform in the lack of distributed charge. On the contrary, some recent results (18) concerning the conduction mechanism for oxides indicate the presence of large quantities of trapped charges in the oxide. If this is so, then on the average, the resistivity of the oxide can be a constant, but the local field in the oxide does not necessarily have to be constant. Therefore, as the oxide becomes thicker, the field nonuniformities can become appreciable; and a stage is finally reached where nonuniform oxide growth will occur. The authors realize, however, that this is not the full explanation of the nonuniform coloration on the 200V samples. As was mentioned earlier, films grown at applied biases up to about 180V for GaAs and 125V for GaP in acidic baths had constant refractive indexes (1.81 and 1.60, respectively), but above this voltage range the apparent refractive index began to deviate markedly from these values (see Fig. 10). We believe this deviation is due to the formation of a peculiar interface region, which is neither well defined nor well understood, but which interferes with a good specular reflection from the oxide-semiconductor interface.

In the analysis presented here, all of the charge carriers in the anodization system have been treated identically, and differentiating between electronic and ionic current has been avoided. Obviously, simplification has been employed again in order to make the problem tractable. Because the specific ionic species moving in and through the oxides are not known (from either the semiconductor or the electrolyte side), it would be foolhardy to attempt an in-depth analysis of the drift effects that most assuredly play a role in the anodic oxidation of these materials. However, the following can be done as a first attempt in this direction. The field across the oxide that causes ionic drift of the oxidant is

$$E_o = \frac{V_o}{d} \quad [11]$$

where  $d$  is the thickness of the oxide. Note that the slope of the thickness vs. applied bias curves (see Fig. 3 and 9) is  $d/V_o$ , the slopes being 20 and 12 A/V for GaAs and GaP, respectively. In obtaining the data for Fig. 3 and 9, heavily doped material (i.e.,  $\sim 1 \times 10^{18} \text{ cm}^{-3}$ ) was used and therefore  $V_B$  was approximately  $\leq 10\text{V}$  (17). Because high-conductivity solutions were used,  $V_s$  can be expected to be negligibly small. Therefore, at  $t = \infty$  under constant voltage conditions

$$V_o = V_A - 10 \quad [12]$$

but at high applied voltages

$$V_o \approx V_A \quad [13]$$

and one can therefore write

$$E_o = \frac{1}{V_o} \cong (\text{slope})^{-1} \quad [14]$$

This means, then, that for GaAs and GaP,  $E_o \cong 5 \times 10^6$  and  $8 \times 10^7 \text{ V/cm}$ , respectively, and one might consider these to be the critical fields necessary for oxide growth to take place.

It is hoped that some future studies will help to elaborate the details of the mechanisms interactive in this area.

#### Conclusions

Information is reported regarding the anodization of GaAs and GaP in aqueous solutions, whereby one can obtain either controlled oxide growth or controlled electrolytic etching. By replacing the older (i.e., aqueous  $\text{H}_2\text{O}_2$ ) approach with the simpler, cheaper water system, one eliminates the problems of spontaneous electrolyte decomposition at the platinum cathode. Also, because of the absence of gas generation, the need for the baffle between the anode and the cathode has disappeared and apparatus requirements have been simplified still further. In addition, since one no longer need purchase a commercial product (i.e.,  $\text{H}_2\text{O}_2$ ) from an outside vendor, it is now possible to have total control of all aspects of the electrolyte preparation.

The influence of a graded region at the semiconductor oxide interface is seen in the anomalous ellipsometry values obtained on samples grown at high voltages. More work will have to be done in order to explain these effects.

#### Acknowledgments

The authors would like to extend sincere thanks to the many colleagues whose discussions and comments

were helpful to us. We especially wish to thank D. L. Rode for his analysis that led to the development of the  $I$ - $V$ - $t$  equations, D. E. Aspnes for his assistance with ellipsometry problems, E. H. Nicollian for discussions on the charge in the oxide, F. K. Reinhart and W. C. Niehaus for discussions regarding the depletion layers at the two oxide interfaces, D. L. Deppen for his preparation of the photoresist pattern used in restricted-area oxidations, and A. P. Pisarchik for his general help on this project.

Manuscript submitted Sept. 29, 1975; revised manuscript received Feb. 9, 1976. This was Paper 282 presented at the Miami Beach, Florida, Meeting of the Society, Oct. 8-13, 1972.

Any discussion of this paper will appear in a Discussion Section to be published in the June 1977 JOURNAL. All discussions for the June 1977 Discussion Section should be submitted by Feb. 1, 1977.

Publication costs of this article were partially assisted by Bell Laboratories.

#### REFERENCES

1. B. Schwartz and W. J. Sundburg *This Journal*, **120**, 576 (1973).
2. R. A. Logan, B. Schwartz, and W. J. Sundburg, *ibid.*, **120**, 385 (1973).
3. S. M. Spitzer, B. Schwartz, and G. D. Weigle, *ibid.*, **122**, 397 (1975).
4. F. Ermanis and B. Schwartz, *ibid.*, **121**, 1665 (1974).
5. R. L. Hartman, B. Schwartz, and M. Kuhn, *Appl. Phys. Letters*, **18**, 304 (1971).
6. B. Schwartz, J. C. Dymant, and S. E. Haszko, "Gallium Arsenide and Related Compounds 1972," p. 187, The Institute of Physics, London (1973).
7. S. M. Spitzer, B. Schwartz, and G. D. Weigle, *This Journal*, **121**, 820 (1974).
8. J. M. Poate, P. J. Silverman, and J. Yahalom, *J. Phys. Chem. Solids*, **34**, 1847 (1973).
9. N. N. Axelrod, H. J. Levinstein, and W. Royer, Private communication.
10. W. C. Niehaus and B. Schwartz, Submitted to *Solid State Electron.*
11. R. J. Archer, *J. Opt. Soc. Am.*, **52**, 970 (1962).
12. D. E. Aspnes, *Opt. Comm.*, **8**, 222 (1973).
13. R. L. Field, Jr., Private communication.
14. H. Gerischer, *Ber. Bunsenges*, **69**, 578 (1965).
15. "Handbook of Chemistry and Physics," 50th ed., R. C. Weast, Editor, Chemical Rubber Co., Cleveland (1969).
16. D. L. Rode, J. V. DiLorenzo, and B. Schwartz, *Solid State Electron.*, **17**, 1119 (1974).
17. S. M. Sze, "Physics of Semiconductor Devices," p. 24, John Wiley & Sons, Inc., New York (1969).
18. E. H. Nicollian and B. Schwartz, To be published.
19. H. E. Phillips, *J. Chem. Soc., London*, **95**, 59 (1909).
20. A. A. Noyes, *J. Am. Chem. Soc.*, **30**, 335 (1908).
21. H. T. S. Britton, *J. Chem. Soc.*, 614 (1927).
22. H. Falkenhagen, "Electrolytes," Clarendon Press, Oxford (1934).

## Appendix B: SLAC Tests of the Anodization Process

The following is a description of anodization tests carried out at SLAC; it has been transcribed (with minor editorial corrections) from a SLAC internal memorandum from T. Roder to C. K. Sinclair dated 9/29/82.

Herewith is a description of the anodization process used by our laboratory to protect and/or clean the surface of epitaxially grown GaAs wafers. This process, documented by Schwartz et al. in *J. Electrochem. Soc.*, **123**, 1089 (July 1976), consists of anodizing the GaAs in a 2.5 pH solution of phosphoric acid at a rate of about 20 Å/V.

The anodization was carried out in a 100 ml Pyrex beaker which had been washed with Deconex and rinsed three times with distilled water in the ultrasonic cleaner. The cathode was fashioned from a 2 mil platinum wire shaped into a 1 inch diameter loop, which was then suspended from the edge of the beaker by a length of the same platinum wire. The GaAs wafer was held in pair of metal tweezers whose tips had been sheathed with small wedges of 1100 aluminum so that no other metals except platinum and aluminum would come in contact with the anodizing solution. Before being used to hold GaAs wafers, these aluminum tips were anodized at 60 volts in the phosphoric acid solution, so that their reaction with the solution would not generate an additional current during the anodization of the GaAs. Electrical contact to the GaAs wafers was assured by scraping away with a scalpel blade, small areas of aluminum oxide on the inside of the tweezer tips.

The anodization solution was mixed by adding two drops of phosphoric acid to approximately 800 cc of distilled water; the pH of the distilled water and of the solution – 6.5 and 2.5 respectively – was measured with a pH- meter. The solution was stored in a polyethylene bottle. Early attempts at measuring precise values of pH with pH paper proved to be unsatisfactory and the use of the latter for this purpose is to be discouraged.

Zn-doped GaAs wafers, that had been bromine-etched and stored in a desiccator for an indeterminate period, were cleaned by the conventional procedure used in our lab – solvents, sulfuric acid, HF, peroxides, and sodium hydroxide – and anodized at 25, 37.5, and 50 volts. The wafer-to- cathode distance was maintained at less than 1/4 inch, and the wafers were fully immersed in the anodizing solution. The current was monitored with a milliammeter and allowed to reach its minimum value at each voltage; these values ranged from 0.1 ma at 25 volts, to 1.1 ma at 50 volts, and were not linearly related to the anodization voltage. The anodization was deemed to be complete after the current was maintained at its minimum value for one minute, the assumption of completion being encouraged by the observation that no further gas bubbles were being formed at the surface of the GaAs. The voltage was then turned down to zero and the wafers were rinsed in distilled water and ethanol. Because long-term storage was not envisaged for the anodized wafers, no attempt was made to bake them in an inert atmosphere as described in Schwartz's paper.

The anodized films are too thin to be measured by conventional interferometry; how-

Anodization Voltage	Wavelength (nm)	Order	Thickness (Å)
50	242.5	2	1055
	385	1	1070
37.5	227.5	3/2	743
	480	1/2	667
25	246.5	1	536
	345	1/2	479

ever, their uniform, brilliant colors suggested the possibility that their thickness could be calculated if the wavelengths of these colors were known. We therefore used the Beckman spectrophotometer to measure the surface reflectance of the films between 220 and 1600 nm. These recordings show that:

1. No detectable peaks occurred above 750 nm;
2. The sample anodized at 50 V, whose color was dark gold, produced a second-order maximum at 242.5 nm, and a first-order maximum at 385 nm;
3. The sample anodized at 37.5 V, whose color was light blue, produced a 3/2-order minimum at 227.5 nm, and a 1/2-order minimum at 480 nm;
4. The sample anodized at 25 V, whose color was dark blue, produced a first-order maximum at 246.5 nm, and a 1/2-order minimum at 345 nm.

The film thickness,  $t$ , was calculated from these values using the relation  $t = (\text{order}) \times \text{wavelength}/2n$ , where  $n$  is the index of refraction of the oxide. While this simple relation does not take into account the phase shift arising at the substrate-oxide interface, as discussed by Pliskin in *Solid-State Elec.* **11**, 957 (1968), a measure of this phase shift can be obtained by calculating the thicknesses at a relatively constant wavelength. The variation of the refractive index with wavelength is thus eliminated and the phase shift can then be determined directly from a plot of thickness vs. anodization voltage.

Two wavelength regions were selected for this purpose: 246.5 nm; and 385 nm. The index of refraction at these two wavelengths was obtained from a paper by Aspnes et al., (*JAP* **48**, 3510 (August 1977)), as follows:  $n=1.8$  at 246.5 nm; and  $n=2.3$  at 385 nm. The calculated oxide film thicknesses are tabulated below:



These points are plotted and two best-fit lines are drawn, one for each wavelength set. Their slope is a measure of anodization rate, and their intercept is used to calculate the phase shift by means of the relation:  $2(p) \times \text{intercept}/\text{wavelength}$ . The short-wavelength line has a slope of  $20 \text{ \AA}/\text{V}$  and a phase shift of zero degrees, while the other has a slope of  $24.2 \text{ \AA}/\text{V}$  and a phase shift of  $-18.6$  degrees.

The results, in particular the ones obtained at the shorter wavelengths, are sufficiently reliable for confident use of this anodization process in our lab.

## Appendix C: Cleaning the NPL Deionized Water System

The NPL deionized water system consists of a Barnstead Nanopure D4741 water treatment system which is fed water that has been pre-treated by passing through a Culligan U-68 mixed bed deionizing filter. If the deionized water system has not been used recently, it should be cleaned according to the following procedure:

1. Save 15 gallons of deionized water from the system.
2. Remove the old filters from the system and discard them (following the procedure in the Barnstead manual).
3. Make up the following disinfecting solutions:
  - (a) Bleach: Add 1 liter of bleach (5.25% sodium hypochlorite) to 15 liters of deionized water to make a 0.3% solution.
  - (b) Hydrogen peroxide: Add 1/2 liter of 30%  $H_2O_2$  to 15 liters of deionized water.
4. Circulate each solution separately, starting with the bleach solution, for 20 to 30 minutes.
5. Discard the  $H_2O_2$  solution through the auxiliary draw off line. (**DO NOT RINSE SYSTEM**)
6. Install new filters (Cole Palmer 1505-24,1505-26) following the Barnstead Procedure.
7. Check Culligan mixed bed pre-treatment filter. The "line purity" lamp should be lit brightly. If it is not lit or very dim call Culligan and have the filter replaced.
8. Run system for several days prior to etching, dispensing water through the auxiliary draw-off several times per day.

## Appendix D: Glassware Cleaning Procedure

1. Start with all new glassware.
2. Ultrasonically clean each item three times using a solution of Alconox in deionized water.
3. Rinse each item out with methanol.
4. Leach each item with boiling deionized water and cover with clean aluminum foil.

## Appendix E: Etching Solution Preparation

Note that solutions should be mixed fresh each time the procedure is to be used. About 50 cc of each solution are required for each crystal.

### 1. $\text{H}_2\text{SO}_4$ :

Mix a 4:1:1 solution of sulfuric acid, 30%  $\text{H}_2\text{O}_2$  and water as follows:

- (a) Rinse 2 400 ml Pyrex beakers with sulfuric acid.
- (b) Pour just over 200 ml of  $\text{H}_2\text{SO}_4$  into one of the 400 ml beakers.
- (c) Fill the other 400 ml beaker with 50 ml of water and 50 ml of  $\text{H}_2\text{O}_2$ , and place the beaker in a large Pyrex dish full of ice. Insert a thermometer in the solution to monitor its temperature.
- (d) Slowly add 200 ml of  $\text{H}_2\text{SO}_4$  to the  $\text{H}_2\text{O}_2$  and water solution. **Do not let the solution temperature rise above 80 C.**

### 2. HF Acid:

- (a) Rinse a 400 ml nalgene tripour beaker with HF.
- (b) Fill beaker with 100 ml of HF.

### 3. NaOH:

- (a) Half fill a 400 ml nalgene tripour beaker with water.
- (b) Dissolve a few NaOH pellets in it, then rinse it out.
- (c) Weigh 4 grams of NaOH pellets into the beaker.
- (d) Add 100 ml of deionized water and wait for the pellets to dissolve.  
(1N NaOH = 4 grams/100 ml)
- (e) Add 100 ml of 30%  $\text{H}_2\text{O}_2$ .